

Research Article

## Biosynthesis of Silver Nanoparticles from *Microsorium Punctatum* (L.) Copel Fronds Extract and an *In-vitro* Anti-Inflammation Study

Philippe Belle Ebanda Kedi<sup>1,2</sup>, Chick Christian Nanga<sup>3</sup>, Awawou Paboudam Gbambie<sup>4</sup>, Vandi Deli<sup>3</sup>, Francois Eya'ane Meva<sup>3,5\*</sup>, Hamza Elsayed Ahmed Mohamed<sup>2,6</sup>, Agnes Antoinette Ntoumba<sup>1</sup>, Moise Henri Julien Nko'o<sup>3,7</sup>, Ülkü Kökçam-Demir<sup>5</sup>, Bastian Moll<sup>5</sup>, Houatchaing Kouemegne Armelle Michelle<sup>3</sup>, Peter Teke Ndifon<sup>4</sup>, Emmanuel Albert Mpondo Mpondo<sup>3</sup>, Alain Bertrand Dongmo<sup>1</sup>, Christoph Janiak<sup>5</sup>, Malik Maaza<sup>2,6</sup>

<sup>1</sup>Department of Animal Biology and Physiology, University of Douala, Douala, Cameroon

<sup>2</sup>Nanosciences African Network (NANOAFNET), iThemba LABS-National Research Foundation, Cape town, South Africa

<sup>3</sup>Department of Pharmaceutical Sciences, University of Douala, Douala, Cameroon

<sup>4</sup>Department of Chemistry, Laboratory of coordination chemistry, University of Yaounde I, Yaounde, Cameroon

<sup>5</sup>Institute for Inorganic Chemistry and Structural Chemistry, Heinrich-Heine-University Düsseldorf, Düsseldorf, Germany

<sup>6</sup>UNESCO-UNISA Africa Chair in Nanosciences and Nanotechnology, College of Graduate Studies, University of South Africa, Pretoria, South Africa

<sup>7</sup>Department of Chemistry, Faculty of Sciences, University of Douala, Douala, Cameroon

**\*Corresponding Author:** Francois Eya'ane Meva, Institute for Inorganic Chemistry and Structural Chemistry, Heinrich-Heine-University Düsseldorf, Düsseldorf, Germany, E-mail: [mevae@daad-alumni.de](mailto:mevae@daad-alumni.de)

**Received:** 17 March 2020; **Accepted:** 26 March 2020; **Published:** 07 April 2020

**Citation:** Philippe Belle Ebanda Kedi, Chick Christian Nanga, Awawou Paboudam Gbambie, Vandi Deli, Francois Eya'ane Meva, Hamza Elsayed Ahmed Mohamed, Agnes Antoinette Ntoumba, Moise Henri Julien Nko'o, Ülkü Kökçam-Demir, Bastian Moll, Houatchaing Kouemegne Armelle Michelle, Peter Teke Ndifon, Emmanuel Albert Mpondo Mpondo, Alain Bertrand Dongmo, Christoph Janiak, Malik Maaza. Biosynthesis of Silver Nanoparticles from *Microsorium Punctatum* (L.) Copel Fronds Extract and an *In-Vitro* Anti-Inflammation Study. Journal of Nanotechnology Research 2 (2020): 025-041.

## Abstract

The present study reports a cost-effective and eco-friendly silver nanoparticles synthesis using *Microsorium punctatum* frond extract as a new solution in the development of therapeutic strategies against inflammation. Egg albumin denaturation model was used to ascertain the anti-inflammatory potential of the biosynthesized silver nanoparticles. Plasmon resonance surface peaked at 440 nm and particles interface were coated with organics. X-ray diffraction pattern showed nanocrystallite nature of 20.05 nm and 39.46 nm size for silver and silver chloride, respectively while the hydrodynamic diameter size was found to be  $29.7 \pm 9.7$  nm. Elemental mapping reveals particles consisting of silver, chloride or carbon among main elements. Highly aggregated and polydispersed spherical silver grain of 10-45 nm size were depicted with electron microscopy. Biosynthesized nanoparticles significantly inhibited thermally induced albumin denaturation indicating their capability to control protein denaturation involved in the inflammatory process thus, plausibly account for the pharmaceutical use of the plant.

**Keywords:** Biosynthesis; Silver nanoparticle; *Microsorium punctatum* extract; Anti-inflammation

## 1. Introduction

Size effects constitute a fascinating aspect of nanomaterials. One of the most direct effects of reducing the size of materials to the nanometer range is the appearance of quantization effects due to the confinement of the movement of electrons, this leads to discrete energy levels depending on the size and structure, thereby creating properties different from those of corresponding bulk materials [1]. The effects determined by size pertain to the evolution of structural, thermodynamic, electronic, spectroscopic, electromagnetic and chemical features of these finite systems with increasing size [2]. These properties are

the consequence of a large number of surface atoms and three-dimensional quantum confinement of electrons, which are believed to be the factors regulating the physical and chemical properties of metal nanoparticles [3]. The synthetic process for metallic nanoparticles can tailor the material through specific application by controlling size and shape distributions.

Plant extract mediated synthesis of nanoparticles is a simple, environment friendly and cost-effective bottom-up technique. It allows subsequent manipulations of the physical-chemical environment through plant secondary metabolites as reducing and stabilizing agent preventing the formation of larger molecules [4]. Nanoparticles have drawn increasing interest in nanomedicine for their ability to deliver drugs in the optimum dosage range often resulting in increased therapeutic efficiency of the drugs, weakened side effects and improved patient compliance [5]. The biological activity of silver nanoparticles depends on various factors including surface chemistry, size, size distribution, shape, particle morphology, particle composition, coating/capping, agglomeration, dissolution rate, particle reactivity in solution, efficiency of silver ion release and cell type [6, 7]. The biogeneration of nanoparticles using plant extracts as reducers might be considered as an effective beneficiary approach for the pharmaceutical industry as the method is not expensive, not cumbersome, eco-friendly and the particles can be subsumed into antimicrobial applications, cosmetic products, packaging.

*Microsorium punctatum* (L.) Copel (Polypodiaceae) is a common fern species found in Africa and Asia, in various forest types of tropics and subtropics from sea level up to 2800 m elevation [8, 9]. The plant is a common medium sized epiphytic herb occurring naturally in semi exposed as well as shaded sites. This specie is cultivated as an ornamental plant and for

medicinal purpose. The plant's crude extract is folklorically used as purgative, diuretic and for wound healing [10, 11]. The plant's leaves are consumed as edible vegetable [12]. Phytochemical screening and pharmacological investigation pointed out their rich phenolic and flavonoid content associated to significant antioxidant and anti-inflammatory activities [13]. The present study therefore reports for the first time, the synthesis and characterization of silver nanoparticles using *Microsorium punctatum* plant frond extract as a bioreactor. In vitro anti-inflammatory study was carried out in order to establish possible biopharmaceutical use of the generated nanoparticles.

## **2. Materials and Methods**

### **2.1 Ethical considerations**

All experimental procedures were in strict compliance with the approved protocol by the Institutional Ethical Committee of the University of Douala (Protocol approval number CEI-UDo/1399/04/2018/T).

### **2.2 Chemicals and reagents**

All chemicals used in this study were of analytical grade. Silver nitrate ( $\text{AgNO}_3$ ) was purchased from Sigma Aldrich Co Ltd Germany. Diclofenac (R. P. Normapur Prolabo, Paris, France) was used as received. Distilled water was used throughout the reactions. All glass wares were washed with dilute nitric acid ( $\text{HNO}_3$ ) and distilled water, and then dried in hot air oven.

### **2.3 Plant collection and extract preparation**

Fresh fronds of *Microsorium punctatum* (Figure 1) were collected at Bonaberi (4°06'19.3"N 9°37'32.7"E), Littoral region, Cameroon, in December 2017 and authenticated by M. Ngansop Eric at the National Herbarium of Cameroon, Yaoundé, in comparison with a voucher specimen previously deposited (n° 18505/SFR/Cam). The entire freshly collected plant was thoroughly washed with running tap water followed by

distilled water to remove all surface contaminants and finely cut. 10 g of the plant was introduced into a conical flask containing 100 mL preheated distilled water (80°C) and stirred for 5 minutes using hot plate equipped with magnetic stirrer. After cooling at room temperature, the solution was filtered using Whatman paper n°1 and used as *Microsorium punctatum* aqueous extract throughout, being stored at 4°C and used for one week due to gradual loss of plant extract viability for prolonged storage. 10 mL of the freshly prepared aqueous extract was introduced into a petri dish and left overnight in the oven at 45°C resulting in the complete evaporation of the solvent. The extract was weighted and the amount of plant extract present in the initial solution was calculated.

### **2.4 Silver nanoparticles synthesis**

Fresh fronds extract of *Microsorium punctatum* was used as a source for the synthesis of silver nanoparticles following a well-known procedure previously described [14]. Briefly, to 10 mL aqueous extract, 50 mL silver nitrate aqueous solution (1 mM) was added and the arrangement was left at room temperature for the bioreduction process. The mixture was incubated in the dark to minimize the photoactivation of silver nitrate under static conditions until changing color appearance, then centrifuged (Hettich D-7200 Tuttlingen, Germany) at 6000 rpm for 20 min and washed twice with distilled water and once with ethanol 95°. Purified pellets were kept into a petri dish, dried in the oven at 60°C for 24 h and used for characterization and anti-inflammatory studies.

### **2.5 Characterization of silver nanoparticles**

**2.5.1 UV-Visible spectroscopic measurement:** The reduction and formation of silver ions was monitored by measuring UV-Visible spectrum of the reaction mixture (plant extract and silver nitrate solution) at 1 h, 24 h, and 48 h using an UV-visible spectrophotometer

(SPECORD S600, 1 nm resolution). Distilled water was used as a blank.

### **2.5.2 Fourier transform infrared spectroscopy:**

Fourier transform infrared (FTIR) spectrum was recorded at room temperature through potassium bromide pellet method. Samples were grinded with KBr pellets and kept in an infrared path and the spectrum was measured using a Nicolet IS5 model of Thermo scientific operating at a resolution of  $0.4\text{ cm}^{-1}$ .

### **2.5.3 Powder X-ray diffraction:**

Powder X-ray diffraction (PXRD) measurements of purified silver nanoparticles were carried out at ambient temperature using a BRUKER D2 Phaser diffractometer (Cu K [ $\text{\AA}$ ] 1.54182, 30 kV) by preparing a film of the silver-organic nanopowder on a flat, low-background silicon sample holder.

### **2.5.4 Dynamic Light Scattering measurement:**

Particle sizes and size distributions were determined using a Zetasizer (Malvern Nano S Zetasizer) operating with a He-Ne laser at a wavelength of 633 nm. 10-15 measurements were made in each run and each analysis was performed in triplicate.

### **2.5.5 High Resolution-Scanning Electron microscopy and Energy Dispersive X-Ray Spectroscopy:**

The biosynthesized silver nanoparticles were subjected to High Resolution-Scanning Electron microscopy (HR-SEM) for morphology determination. A small amount of sample powder was deposited on a carbon coated carbon grid and coated with carbon using a coating sputter coater (Quorum Q 150 TES) to increase the conductivity of the sample. SEM images were taken using Carl Zeiss Auriga Field Emission Scanning Electron microscope (FEG SEM) image at 5 keV. Energy Dispersive X-ray Spectroscopy (EDS) spectrum for elemental analyses was collected with an Oxford

Instruments X-Max solid-state silicon drift detector operating at 20 keV coupled to a TECNAI G2 HRSEM.

### **2.5.6 High Resolution-Transmission Electron Microscopy and Selected Area Electron Diffraction:**

For the High Resolution-Transmission Electron Microscopy (HR-TEM), the sample was prepared by placing a drop of the nanoparticles suspension on the carbon-coated copper grid and allowing water evaporation inside the vacuum dryer. HR-TEM observations as well as Selected Area Electron Diffraction (SAED) were carried out using an FEI Tecnai G2 Field Emission Gun - HRTEM operating at 200 kV.

### **2.6 Anti-inflammatory activity: heat-induced egg albumin denaturation assay**

The synthesized silver nanoparticles were screened for anti-inflammatory properties using inhibition of albumin denaturation technique as previously described [15]. Briefly, the reaction mixture (5 mL) consisted of 0.2 mL of egg albumin (from fresh hen's egg), 2.8 mL of phosphate buffered saline (PBS, pH 6.4) and 2 mL of varying concentrations of silver nanoparticles (50, 25, 12.5, 6.25, 3.125  $\mu\text{g/mL}$ ). Similar volume of distilled water served as control. The mixture was incubated at  $37^\circ\text{C}$  in a biochemical oxygen demand incubator for 15 min then heated at  $70^\circ\text{C}$  for 5 min. After cooling, their absorbance was measured at 660 nm by using vehicle as blank. Diclofenac was used as reference drug and treated similarly for determination of absorbance. The anti-inflammatory activity was estimated in percentage inhibition of protein denaturation and calculated by using the Equation (1):

$$\% \text{ inhibition} = 100 \times \frac{\text{Abs sample}}{\text{Abs control}} - 1 \quad (1)$$

### **2.7 Statistical analysis**

One-way ANOVA was applied to analyze the variability among various parameters using software

PRISMA (GraphPad Software, Inc., San Diego, CA, version 5.01). All experiments were performed in triplicate.

### 3. Results

#### 3.1% yield of extract

Aqueous extraction of *Microsorium punctatum* fronds yielded 36% (w/v) of the original plant material extracted. The crude extract obtained after complete dryness was a deep-brown, sweet-smelling solid residue.

#### 3.2 Visual observation of biosynthesized silver nanoparticles

A visual observation of a change in colour from clear brown to a darkish solution after adding silver nitrate solution was recorded. Silver nitrate solution, *Microsorium punctatum* fresh fronds extract and silver nanoparticles solution are depicted in Figure 2. The observed changing colour due to formation of Plasmon at the colloid surface occurs 48 h following incubation. No further change was observed indicating the stabilization of the synthesized nanoparticles.



**Figure 1:** *Microsorium punctatum* in its natural milieu.

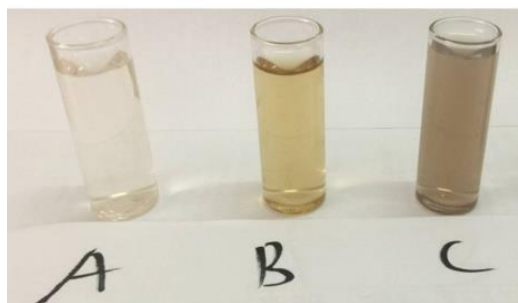


**Figure 2:** (A) Silver nitrate; (B) *Microsorium punctatum* leaf extract; and (C) silver nanoparticles solutions.

#### 3.3 Characterization of biosynthesized silver nanoparticles

**3.3.1 UV-Visible spectroscopy:** The bio-reduction of silver ions in aqueous solution was monitored by

periodic sampling of reaction mixture and subsequently measuring UV visible spectra of the same. The UV-visible spectrum recorded against distilled water as a function of time of reaction is shown on Figure 3. The

characteristic peak of silver nanoparticle known as surface Plasmon resonance confirming the presence of nanoparticles in the sample was observed at 440 nm on the spectra and occurred 48h following incubation.

### 3.3.2 Infrared Spectroscopy of silver nanoparticles from *Microsorium punctatum*:

The Infrared spectrum of silver nanoparticles from *Microsorium punctatum* recorded over the spectral range from 0  $\text{cm}^{-1}$  to 4000  $\text{cm}^{-1}$  is depicted in Figure 4. Characteristics IR peak centred at 1044  $\text{cm}^{-1}$  is associated with a strong sharp C-N stretch. The peak centred at 1223  $\text{cm}^{-1}$  is attributed to stretching mode of C-N bonds. Absorption band at 1392  $\text{cm}^{-1}$  is due to stretching vibration of C-O group. The absorption occurring at 1534  $\text{cm}^{-1}$  can be attributed to N-O nitro compound. The band at 1618  $\text{cm}^{-1}$  is attributed to the stretching vibration mode of C=C bond of unsaturated ketone. The weak broad absorption band at 2165  $\text{cm}^{-1}$  is due to the presence of C $\equiv$ C bonds. The band at 2910  $\text{cm}^{-1}$  represents C-H vibrations of alkane and the broad absorption band at 3390  $\text{cm}^{-1}$  can be attributed to N-H aliphatic primary amine stretch.

**3.3.3 Powder X-ray diffraction results:** The typical powder X-ray diffraction pattern of biosynthesized silver nanoparticles from *Microsorium punctatum* is shown in Figure 5, while their principal characteristics are indicated on table 1 and 2 respectively. The pattern is compatible with the cubic phase of Ag with diffraction points at  $2\theta$  values of 37.17°, 43.37°, 62.92°, and 75.39° that can be indexed to the (111), (200), (220), and (311) planes of the face-centered cubic (fcc) structure respectively (JCPDS file: 65-2871). The pattern also showed the presence of the cubic phase of AgCl at  $2\theta$  values of 27.78°, 32.18°, 46.20°, 54.79°, 57.36°, 67.41°, 74.40°, and 76.93° corresponding to the (111), (200), (220), (311), (222), (400), (311) and (420) planes, respectively (JCPDS file: 31-1238). To determine the average size of synthesized particle, the

most intense peaks of Ag and AgCl were preferred. Thus, (111) and (200) lattice planes of Ag and AgCl have been selected. The calculated average crystalline particle size using the Debye-Scherrer formula was found to be 20.05 and 39.46 nm for silver and silver chloride, respectively. No other characteristic peaks were indicated by the XRD analysis suggesting the high purity of the as-prepared Ag@AgCl nanoparticles.

### 3.3.4 Dynamic Light scattering spectroscopy results:

Particles size and size distributions of the synthesized silver nanoparticles using dynamic light scattering technique are depicted in Figure 6. It is observed that the particles obtained have a good dispersion with hydrodynamic diameters of 50.45 nm. The size distribution of the synthesized silver nanoparticles using *Microsorium punctatum* extract are reported in the Figure below by volume (Figure 6), by intensity (Figure 7) and by number (Figure 8).

### 3.3.5 Scanning Electron Microscopy and Energy Dispersive X-ray Spectroscopy results:

Figure 9A depicts the HR-SEM image of silver nanoparticle synthesized using *Microsorium punctatum* aqueous extract. It is noticeable that almost all the nanoparticles are highly crystalline aggregates of spherical shape with varied size. The energy dispersive x-ray (EDS) analysis gives qualitative as well as quantitative status of elements that may be involved in formation of nanoparticles thus, confirms the presence of silver as shown in Figure 9B. The EDS spectrum of biosynthesized silver nanoparticle shows an intense optical absorption band peak at 2.6 and 3 keV corresponding to chloride and silver respectively (Figure 9B). The elemental profile of synthesized nanoparticles is resumed on Table 3. The peaks situated at the binding energy of 0.2 and 0.5, keV belonging to carbon and oxygen respectively are from the biomolecules bound to the surface of the silver

nanoparticles and/or due to sample grid holder which is made from carbon.

### 3.3.6 HR-Transmission Electron Microscopy and selected area electron diffraction results:

High resolution transmission electron microscopy (HR-TEM) images at different resolutions (Figure 10A), show polydispersed spherical shaped silver nanoparticles with various size. The size distribution when a section of these nanoparticles is considered is depicted in Figure 10B. Figure 10C shows the selected area electron diffraction (SAED) pattern of the synthesized nanoparticles. The ring-like diffraction pattern indicates that the particles are crystalline. The diffraction rings

could be indexed on the basis of the silver and silver chloride mixture.

### 3.4 Inhibition effect of silver nanoparticles from *Microsorium punctatum* on albumin denaturation

Synthesized silver nanoparticles from *Microsorium punctatum* effects on heat-induced egg albumin denaturation are summarized on Table 4. All tested concentrations significantly inhibited the denaturation of egg albumin in a concentration-dependent manner. The gotten maximum inhibition percentage was 69% at the highest tested concentration (100  $\mu\text{g}/\text{mL}$ ). Also, diclofenac used as standard drug exhibited an inhibition of 81% at the concentration of 100  $\mu\text{g}/\text{mL}$ .

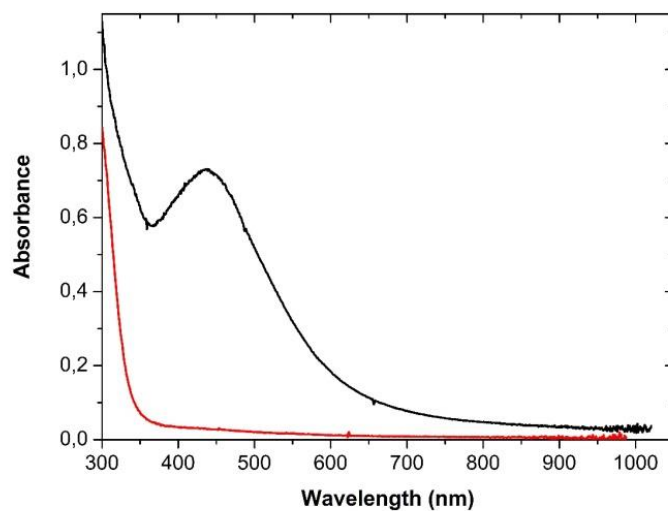


**Figure 3:** UV-Visible spectrum of silver nanoparticles from *Microsorium punctatum* at 48 hours.

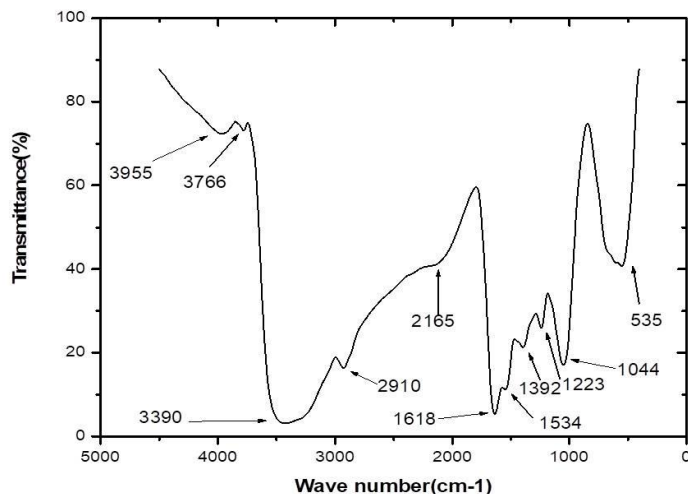


Figure 4: Fourier Transformed Infrared spectrum of silver nanoparticles from *Microsorium punctatum*.

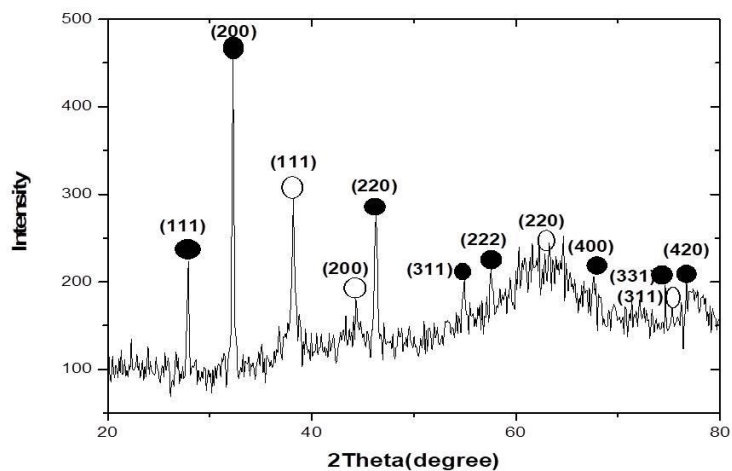


Figure 5: X-ray diffractogram pattern of silver nanoparticles from *Microsorium punctatum*.

S. No.	Position [°2Theta]	Peak height [cps]	FWHM [°2Theta]	Surface [cts*°2Theta]	Miller indices	Ag/AgCl
1	27.78	382	0.2190	546.7	(111)	AgCl
2	32.18	1000	0.2190	1080.3	(200)	AgCl
3	37.17	230.9	0.2190	402.8	(111)	Ag
4	43.37	207.8	0.2190	189.4	(200)	Ag
5	46.20	647.4	0.2190	539.0	(220)	AgCl

6	54.79	339.5	0.2190	107.8	(311)	AgCl
7	57.36	388.9	0.2190	130.4	(222)	AgCl
8	62.92	561.6	0.2190	105.0	(220)	Ag
9	67.41	396.3	0.2190	42.9	(400)	AgCl
10	74.40	262.4	0.2190	16.9	(331)	AgCl
11	75.39	271.5	0.2190	111.2	(311)	Ag
12	76.93	457.9	0.2190	86.2	(420)	AgCl

**Table 1:** Principal characteristic values for the X-ray diffractogram of silver nanoparticles from *Microsorum punctatum*.

	Phase composition (%)	Particles size (nm)
Ag	84.4	20.05
AgCl	15.6	39.46

**Table 2:** Phase composition and calculated particles size of silver nanoparticles from *Microsorum punctatum*.

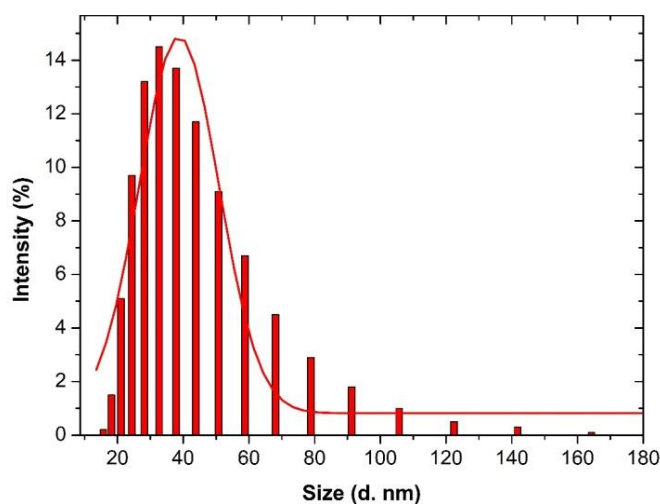


**Figure 6:** Histogram and Gaussian fit of *Microsorum punctatum* silver nanoparticles size distribution by volume from dynamic light scattering measurement.

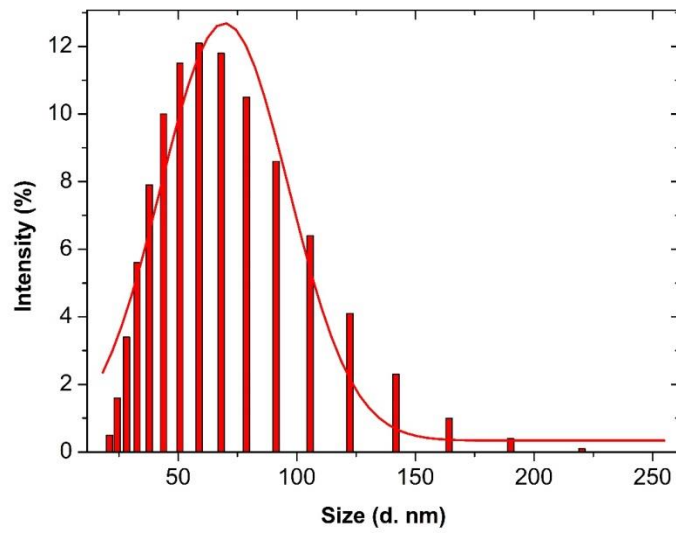


**Figure 7:** Histogram and Gaussian fit of *Microsorium punctatum* silver nanoparticles size distribution by intensity from dynamic light scattering measurement.

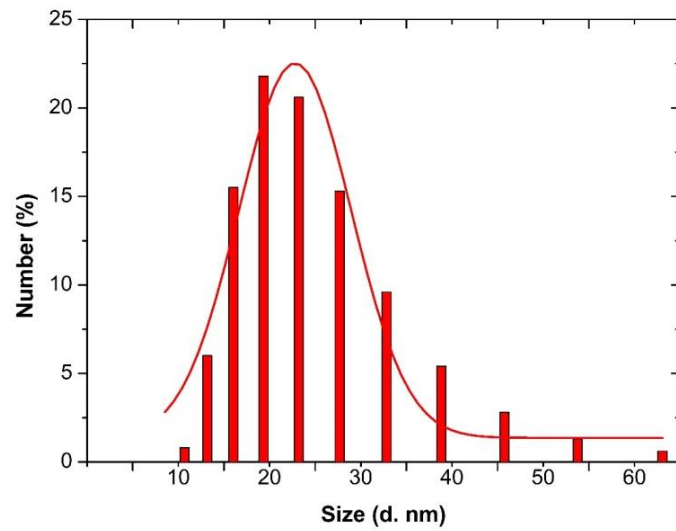
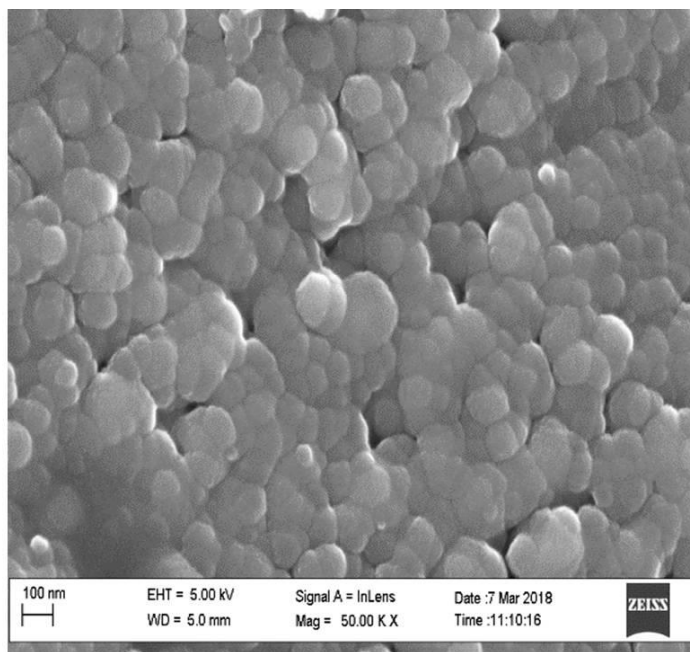
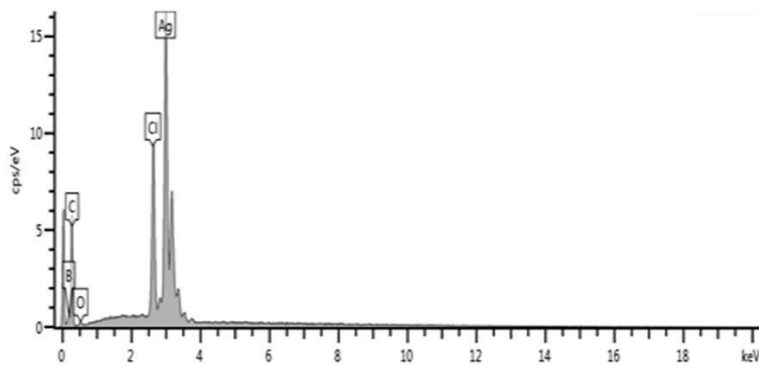


**Figure 8:** Histogram and Gaussian fit of *Microsorium punctatum* silver nanoparticles size distribution by number from dynamic light scattering measurement.



(A)

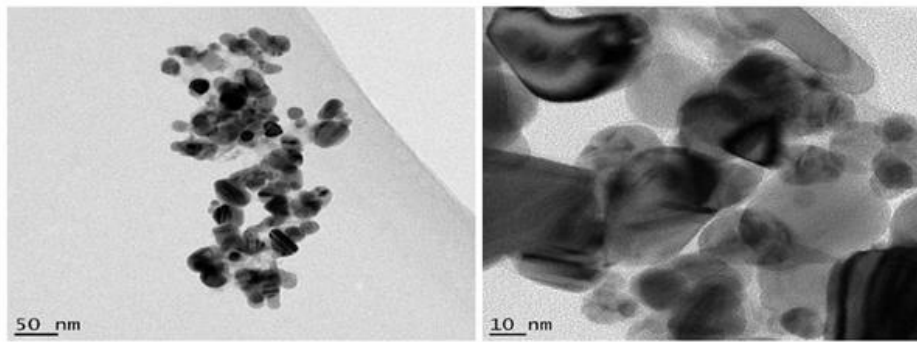


(B)

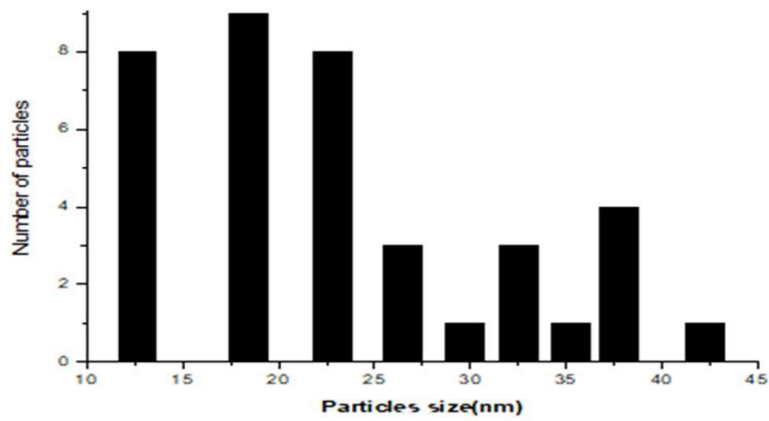
Figure 9: (A) HR-SEM images; and (B) EDS spectrum of silver nanoparticles from *Microsorium punctatum*.

Elements	% Atomic
C	74.52
O	2.37
Cl	7.89
Ag	15.22
<b>Total</b>	<b>100</b>

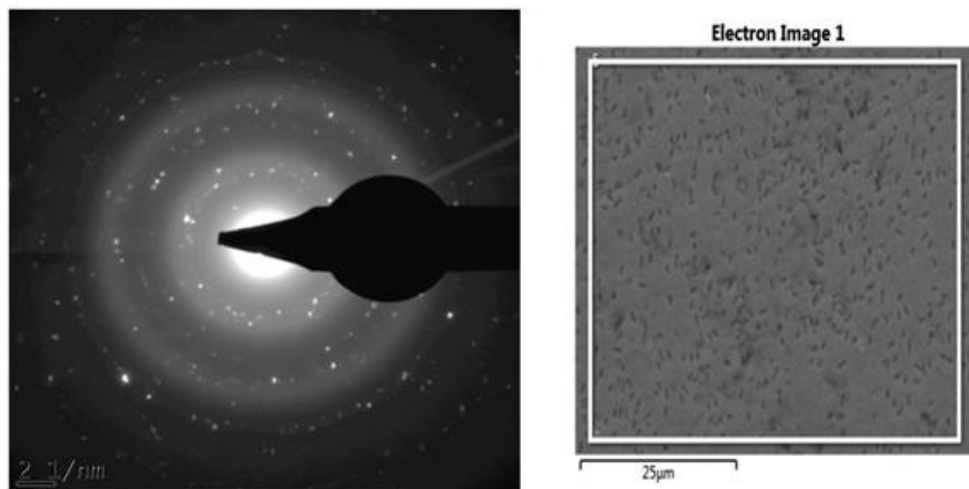
Table 3: Elemental composition of silver nanoparticles from *Microsorium punctatum*.



(A)



(B)



(C)

**Figure 10:** (A) HR-TEM images of the silver nanoparticles from *Microsorium punctatum* ; (B) Size distribution using a section of silver nanoparticles; (C) SAED pattern of silver nanoparticles from *Microsorium punctatum*.

Sample	Concentration ( $\mu\text{g/mL}$ )	% inhibition	IC <sub>50</sub> ( $\mu\text{g/mL}$ )	Logarithmic equation
Control	-	-	16.05	$y = 10.82 \ln(x) + 19.97$
MP-AgNPs	100	69		
MP-AgNPs	50	67		
MP-AgNPs	25	52		
MP-AgNPs	12.5	47		
MP-AgNPs	6.25	39		
Diclofenac	100	81	5.43	$y = 12.69 \ln(x) + 28.53$
Diclofenac	50	79		
Diclofenac	25	77		
Diclofenac	12.5	67		
Diclofenac	6.25	43		

**Table 4:** Influence of silver nanoparticles from *Microsorium punctatum* and Diclofenac against albumin denaturation.

#### 4. Discussion

The synthesis of silver nanoparticles by a cost-effective and environmental friendly pathway using the plant frond extract of *Microsorium punctatum* is described. Biogenerated silver anti-inflammation property is demonstrated. Visual observation of changing color of the reaction mixture (plant extract and silver nitrate) 48 hours following incubation from clear brown to darkish at the end of the reaction was first recorded. This changing color is due to the formation of plasmon at the colloid surface, due to coherent oscillation of conduction electrons on the surface indicating the formation of nanoparticles [16]. Uv-vis spectroscopy is a widely used technique to characterize the optical properties of nanoparticles. The method allows formation and stability study [17]. The UV-visible spectra recorded against water as a function of time illustrated the characteristic peak of plasmon resonance surface at 440 nm confirming the synthesis and stability of silver nanoparticles. Thus, *Microsorium punctatum* aqueous extract acts as a reductant as well as capping

agent. Such have been observed for olive leaf extract [17].

To study the surface functionalization at the nanoparticle-metabolite interface, a typical FTIR spectrum of the synthesized silver nanoparticles has been obtained. The potential biomolecules responsible for the reduction, capping and stability of the synthesized silver nanoparticles were associated with absorption bands of various stretching modes including NH, CH, CC, CN, NO and CO. FTIR analysis shows evidence that the silver nanoparticles are capped with phytochemicals with various functional groups of organic molecules giving characteristic peaks in the spectrum. Similar observations have been reported while using *Stachytarpheta cayennensis* aqueous extract as bioreactor [18].

XRD is one of the most important characterization techniques to reveal the structural properties of nanoparticles. It gives enough information about the crystallinity and phase of the nanoparticles. X-ray

diffraction patterns of nanomaterials provide a wealth of information - about phase composition, crystallite size, lattice strain, and crystallographic orientation [4, 19]. The typical PXRD pattern of the prepared nanoparticles presented in Figure 5 is compatible with the cubic phase of silver with various diffraction points corresponding to the fcc structure (JCPDS file: 65-2871). The PXRD pattern also showed the presence of the cubic phase of silver chloride (JCPDS file: 31-1238). No other characteristic peaks were found, indicating the high purity of the as-prepared silver and silver chloride nanoparticles. The most intense peaks of silver and silver chloride were chosen to calculate the average crystalline particle size [20]. Thus, we selected the (111) and (200) lattice planes of silver and silver chloride, respectively. Mean particles sizes of 39.46 nm was obtained for silver chloride while 20.05 nm was obtained for silver. Similar observations were made using extracts of *Selaginella myosorus*, *Corchorus olitorius* or *Ipomea batatas* [14, 21]. It was possible to obtain a phase composition quantification of 84.4% for silver chloride and 15.6% for silver.

Dynamic light scattering (DLS) is a technique for characterizing the size of colloidal dispersions which utilizes the illumination of a suspension of particles or molecules undergoing Brownian motion by a laser beam. In fact, when a particle is illuminated with a laser, the intensity of the scattered light fluctuates at a rate that is dependent upon the particle size. The sizes using DLS accounts with nanoparticles and molecules adsorbed or electrostatically bounded [22]. This quality is fundamental for biopharmaceutical uses. In this study, the synthesized silver nanoparticles size determined using DLS technique was found to be 50.45 nm. The control of size dimensions in solution is critical when plant extracts are considered. The metallic nanoparticles generated tend to agglomerate due to Brownian motion. The DLS data obtained in the case *Microsorium*

*punctatum* silver nanoparticles are of good quality thus plant secondary metabolites are able to stabilize effectively the particles in solution. The dispersion is good enough for data collection and analysis which enable a cumulative study. Less large or sedimenting particles are therefore formed.

The detailed size and morphology of the nanoparticles have been investigated using HR-SEM and HR-TEM coupled with EDS and SAED, respectively. The synthesized silver nanoparticles studied with HR-SEM were found spherical and aggregated. HR-TEM microscopy shows particles with 10-45 nm size. Sizes obtained by powder X ray diffraction analysis are inside that range (39.46 nm for silver chloride, 20.05 nm for silver) while DLS size is 50.45 nm. Silver nanoparticles have the tendency to agglomerate due to their high surface tension of ultrafine nanoparticles [23]. The fine particle size results in a large surface area that, in turn, enhances the nanoparticle activities. The EDS profile of bio-reduced silver ions indicated that the silver nanoparticles contain pure silver, carbon and oxygen due to the presence of secondary metabolites and chloride from silver chloride nanocrystallites [24]. SAED pattern clearly confirmed their crystalline nature of both nanograins.

In the present study, the protein denaturation bioassay was selected for *in-vitro* assessment of anti-inflammatory property of synthesized silver nanoparticles. Protein denaturation is one of the well documented causes of inflammatory and arthritic diseases [25]. It has been reported that production of auto-antigens in certain arthritic diseases may be due to denaturation of tissue protein *in vivo* [26]. In inflammatory-related diseases, soluble proteins and peptides are converted into highly organized fibrillar aggregates. The accumulation of abnormal protein and peptide aggregates exerts toxicity by disrupting

intracellular transport, overwhelming protein degradation pathways and/or disturbing vital cell functions [27]. Thermal denaturation of albumin leads to the exposure of hydrophobic residues, which increases hydrophobic attraction that overcomes electrostatic repulsion and triggers the aggregation of amorphous aggregates. Silver nanoparticles from *Microsorium punctatum* were effective in inhibiting thermally induced albumin denaturation at different concentrations, as shown in table 5. The effect is slightly lower than diclofenac indicating the capability of the biosilver to control protein denaturation involved in the inflammatory process by opposing to self-aggregation of proteins thus, would be worthwhile for anti-inflammatory drug development.

## 5. Conclusion

In the present study, silver nanoparticles were biogenically synthesized via complete green process without the addition of any material except for the precursor. Developed particles were spherical in shape of various size, polydispersed and crystalline in nature. Anti-inflammatory potency was assessed and the result indicated their effectiveness against protein denaturation. This attempt to highlight the potential pharmaceutical uses of silver nanoparticles from *Microsorium punctatum* provides novel, effective and safe approach to design future anti-inflammatory therapies. Although these compounds are promising, further *in vivo* investigation, preclinical and clinical trials is required in this respect.

## Disclosure

The authors declared having no competing interests.

## Acknowledgments

Authors are thankful to the Multidisciplinary Laboratory of the Faculty of Medicine and Pharmaceutical Sciences, Department of Pharmaceutical Sciences for **Journal of Nanotechnology Research**

technical support. PBEK thanks the African-German Network of Excellence in Science (AGNES) for granting a Mobility Grant in 2017. Support of Word University Service under APA 2668 for providing part equipment used is appreciate. FEM thank the German Academic Exchange Service DAAD for a generous Professor Fellowship (grant no. 768048).

## References

1. Beriso A, Ghoshal SK. Study of dependence of optical parameters on the size of nanoporous silicon quantum dot through energy gap. *Adv Phy Theo App* 72 (2018): 8-19.
2. Rao JP, Geckeler KE. Polymer nanoparticles: preparation techniques and size-control parameters. *Prog Polym Sci* 36 (2011): 887-913.
3. Saion E, Gharibshahi E, Nagavi K. Size-controlled and optical properties of monodispersed silver nanoparticles synthesized by the radiolytic reduction method. *Int J Mol Sci* 14 (2013): 7880-7896.
4. Eya'ane Meva F, Ntoumba AA, Belle Ebanda, et al. Silver and palladium nanoparticles produced using a plant extract as reducing agent, stabilized with an ionic liquid: sizing by X-ray powder diffraction and dynamic light scattering. *J Mater Res Technol* 8 (2019): 1991-2000.
5. Alexis F, Pridgen E, Molnar LK, et al. Factors affecting the clearance and biodistribution of polymeric nanoparticles. *Mol Pharm* 5 (2008): 505-515.
6. Carlson C, Hussain SM, Schrand AM, et al. Unique cellular interaction of silver nanoparticles: size-dependent generation of reactive oxygen species. *J Phys Chem B* 112 (2008): 13608-13619.

7. Jain N, Bhargava A, Majumdar S, et al. Extracellular biosynthesis and characterization of silver nanoparticles using *Aspergillus flavus* NJP08: a mechanism perspective. *Nanoscale* 3 (2011): 635-641.
8. Nooteboom HP. The microsorioid ferns (Polypodiaceae). *Blumea* 42 (1997): 261-395.
9. Petchsri S, Boonkerd T, Baum BR. Phenetic study of the *Microsorium punctatum* complex (Polypodiaceae). *Science Asia* 38 (2012): 1-12.
10. Nayar BK. Medicinal Ferns of India. *Bull Nat Bot Gard* 58 (1957): 1-38.
11. Sharma UK, Pegu S. Ethnobotany of religious and supernatural beliefs of the mising tribes of assam with special reference to the 'Dobur Uie'. *J Ethnobiol Ethnomed* 7 (2011): 16.
12. Benjamin A, Manickam VS. Medicinal pteridophytes from Western Ghats. *IJTK* 6 (2007): 611-618.
13. Dela Cruz RY, Ang AMG, Doblaz GZ, et al. Phytochemical screening, antioxidant and anti-inflammatory activities of the three fern (Polypodiaceae) species in Bukidnon, Philippines. *Bull Env Pharmacol Life Sci* 6 (2017): 28-33.
14. Belle Ebanda Kedi P, Eya'ane Meva F, Kotsedi L, et al. Eco-Friendly synthesis, characterization, in vitro and in vivo anti-inflammatory activity of silver nanoparticle-mediated *Selaginella myosurus* aqueous extract. *Int J Nanomed* 13 (2018): 8537-8548.
15. Chandra S, Chatterjee P, Dey P, et al. Evaluation of anti-inflammatory effect of ashwagandha: a preliminary study in vitro. *Pharmacognosy J* 4 (2012): 47-49.
16. Eya'ane Meva F, Segnou ML, Okalla Ebongue C, et al. Spectroscopic synthetic optimizations monitoring of silver nanoparticles formation from *Megaphrynium macrostachyum* leaf extract. *Rev Bras Farm* 26 (2016): 640-646.
17. Khalil MMH, Ismail EH, El-Baghdady KZ, et al. Green synthesis of silver nanoparticles using olive leaf extract and its antibacterial activity. *Arabian J Chem* 7 (2014): 1131-1139.
18. Eya'ane Meva F, Avom MJO, Okalla Ebongue C, et al. *Stachytarpheta cayennensis* aqueous extract, a new bioreactor towards silver nanoparticles for biomedical applications. *J Biomater Nanobiotech* 10 (2019): 102-119.
19. Theivasanthi T, Alagar M. Electrolytic synthesis and characterizations of silver nanopowder. *Nano Biomed Eng* 4 (2012): 58-65.
20. Awwad AM, Salem NM, Ibrahim QM, et al. Phytochemical fabrication and characterization of silver/silver chloride nanoparticles using *Albizia julibrissin* flowers extract. *Adv Matter Lett* 6 (2015): 726-730.
21. Eya'ane Meva F, Okalla Ebongue C, Fannang SV, et al. Natural substances for the synthesis of silver nanoparticles against *Escherichia coli*: the case study of *Megaphrynium macrostachyum* (Marantaceae), *Corchorus olitorus* (Tiliaceae), *Ricinodendron heudelotii* (Euphorbiaceae), *Gnetum bucholzianum* (Gnetaceae), and *Ipomoea batatas* (Convolvulaceae). *J Nanomater* 2017 (2017): 6834726.
22. Saxena A, Tripathi RM, Singh RP. Biological synthesis of silver nanoparticles by using onion (*Allium cepa*) extract and their antibacterial activity. *Digest J Nanomater Biostr* 5 (2010): 427-432.
23. Annamalai J, Nallamuthu T. Green synthesis of silver nanoparticles: characterization and determination of antibacterial potency. *Appl Nanosci* 6 (2006): 259-265.

24. Anitha P, Sakthivel P. Synthesis and characterization of silver nanoparticles using Delonix Elata leaf extract and its anti-inflammatory activity against human blood cells. *Int J Sci Eng Technol* 4 (2016): 2395-4752.
25. Tooba NS, Romana P, Sumbul A, et al. Trypsin Inhibitors from *Cajanus cajan* and *Phaseolus limensis* Possess Antioxidant, Anti-Inflammatory, and Antibacterial Activity. *J Diet Suppl* 15 (2018): 939-950.
26. Umapathy E, Ndebia EJ, Meeme A, et al. An experimental evaluation of *Albuca setosa* aqueous extract on membrane stabilization, protein denaturation and white blood cell migration during acute inflammation. *J Med Plants Res* 4 (2010): 789-795.
27. Shanker U, Jassal V, Rani M, et al. Towards green synthesis of nanoparticles: from bio-assisted sources to benign solvents. A review. *Int J Env Anal Chem* 96 (2016): 801-835.



This article is an open access article distributed under the terms and conditions of the [Creative Commons Attribution \(CC-BY\) license 4.0](https://creativecommons.org/licenses/by/4.0/)